



HAL
open science

Asymptotic consistency of the RS-IMEX scheme for the low-Froude shallow water equations: Analysis and numerics

Hamed Zakerzadeh

► **To cite this version:**

Hamed Zakerzadeh. Asymptotic consistency of the RS-IMEX scheme for the low-Froude shallow water equations: Analysis and numerics. XVI International Conference on Hyperbolic Problems: Theory, Numerics, Applications, Aug 2016, Aachen, Germany. hal-01520726

HAL Id: hal-01520726

<https://hal.science/hal-01520726>

Submitted on 10 May 2017

HAL is a multi-disciplinary open access archive for the deposit and dissemination of scientific research documents, whether they are published or not. The documents may come from teaching and research institutions in France or abroad, or from public or private research centers.

L'archive ouverte pluridisciplinaire **HAL**, est destinée au dépôt et à la diffusion de documents scientifiques de niveau recherche, publiés ou non, émanant des établissements d'enseignement et de recherche français ou étrangers, des laboratoires publics ou privés.

Asymptotic consistency of the RS-IMEX scheme for the low-Froude shallow water equations: Analysis and numerics

Hamed Zakerzadeh

Abstract In the present work, we *formally* prove the asymptotic consistency of the recently presented Reference Solution IMplicit-EXplicit (RS-IMEX) scheme for the two-dimensional shallow water equations. The scheme has been analyzed extensively for the low-Froude one-dimensional shallow water equations in [Zakerzadeh, *IGPM report 455* (2016)], and the present paper is going to discuss the asymptotic consistency analysis for the two-dimensional case, with the aid of some numerical experiments.

1 RS-IMEX schemes: an introduction

In the singular limits of conservation laws, characterized by the singular parameter $\varepsilon \in (0, 1]$ approaching zero, the type of the equations changes, e.g., when the Mach number, denoted by ε , approaches zero for the Euler equations (the incompressible limit), the sound speed goes to the infinity and the system changes to be hyperbolic-elliptic. Such a singularity not only hinders the analysis (see [16]), but also gives rise to lots of issues for numerical schemes, e.g., schemes may lose their accuracy for under-resolved mesh sizes (see [6]) for weakly compressible flows or the time step gets very restrictive for explicit schemes, in virtue of the Courant–Friedrichs–Lewy (CFL) condition, i.e., $\Delta t \lesssim \varepsilon \Delta x$, which leads to a huge computational cost.

Assuming that the “*solution*” of the singularly-perturbed problem converges to the “*solution*” of the limit problem, we aim to discuss the counterpart of such a convergence in the discrete level. This is the idea of Asymptotic Preserving (AP) schemes [13] for an ε -dependent system converging to a limit for $\varepsilon \rightarrow 0$. The numerical scheme is AP if it provides a stable, consistent, and efficient scheme for the

Hamed Zakerzadeh
Institut für Geometrie und Praktische Mathematik, RWTH Aachen University
Templergraben 55, 52056 Aachen, Germany
e-mail: h.zakerzadeh@igpm.rwth-aachen.de

continuous limit system. For the sake of simplicity, we only consider well-prepared initial data to eliminate spurious initial layers.

The AP property has been studied extensively for conservation laws (as well as kinetic equations, cf. [14]), and several AP schemes have been developed and analyzed; see [2, 17, 5, 12] among others. Although most of these works present a *formal* analysis, there are few results regarding the rigorous asymptotic consistency or stability, e.g., [1, 8, 7, 10, 19] for hyperbolic balance laws.

The bottom-line of these AP schemes is a mixed implicit-explicit (IMEX) approach to split the flux (or its Jacobian) into stiff and non-stiff parts and treat them explicitly and implicitly in time. Such an approach is necessary for an ε -uniform CFL condition, but is not sufficient for asymptotic stability; see [17] for instance, where a *CFL-stable* IMEX scheme requires an ε -dependent time step for stability. This, in fact, gave the motivation for the RS-IMEX scheme, as we will review here. The *penalization method* [9] for the kinetic equations, as well as [2] for the shallow water equations are close to the RS-IMEX scheme, in essence.

The goal of this section is to provide a very brief introduction to the RS-IMEX scheme; see also [18, 15]. Then in the next section, we prove the asymptotic consistency of the scheme followed by some numerical experiments in Section 4. The reader is referred to [18] for a rigorous asymptotic analysis for the one-dimensional shallow water system, which is the backbone of the analysis in the present work.

Consider the general hyperbolic system of balance laws in $\Omega \subset \mathbb{R}^d$

$$\partial_t \mathbf{U}(\mathbf{x}, t; \varepsilon) + \operatorname{div}_{\mathbf{x}} \mathbf{F}(\mathbf{U}, \mathbf{x}, t; \varepsilon) = \mathbf{S}(\mathbf{U}, \mathbf{x}, t; \varepsilon), \quad (1)$$

where $\Omega := \mathbb{T}^d$ is a d -dimensional torus, $\mathbf{U} \in \mathbb{R}^q$ is the vector of unknowns, $\mathbf{F} \in \mathbb{R}^{q \times d}$ is the flux matrix (in d space dimensions), $\varepsilon \in (0, 1]$ is the singular parameter, and $\mathbf{S} \in \mathbb{R}^q$ is the source term. Note that we often suppress the dependence of \mathbf{U} , \mathbf{F} and \mathbf{S} on ε . To have a hyperbolic system, we also assume that \mathbf{F} has a real diagonalizable Jacobian $\mathbf{F}' := \partial_{\mathbf{U}} \mathbf{F}$.

The main idea of the RS-IMEX scheme is to split the solution \mathbf{U} of the balance laws (1) into the (given) reference solution $\bar{\mathbf{U}}$ and a perturbation \mathbf{U}_{pert} , i.e., $\mathbf{U} = \bar{\mathbf{U}} + \mathbf{U}_{pert}$. The reference solution can be a steady state solution of (1), or the solution of the asymptotic limit of (1) as $\varepsilon \rightarrow 0$. Then, as in [18], we use a Taylor expansion around $\bar{\mathbf{U}}$ to split the flux and source terms into reference $(\bar{\mathbf{F}}, \bar{\mathbf{S}})$, linear stiff $(\tilde{\mathbf{F}}, \tilde{\mathbf{S}})$ and non-linear non-stiff parts $(\hat{\mathbf{F}}, \hat{\mathbf{S}})$:

$$\begin{aligned} \mathbf{F}(\mathbf{U}) &= \mathbf{F}(\bar{\mathbf{U}}) + \mathbf{F}'(\bar{\mathbf{U}}) \mathbf{U}_{pert} + (\mathbf{F}(\mathbf{U}) - \mathbf{F}(\bar{\mathbf{U}}) - \mathbf{F}'(\bar{\mathbf{U}}) \mathbf{U}_{pert}) =: \bar{\mathbf{F}} + \tilde{\mathbf{F}} + \hat{\mathbf{F}}, \\ \mathbf{S}(\mathbf{U}) &= \mathbf{S}(\bar{\mathbf{U}}) + \mathbf{S}'(\bar{\mathbf{U}}) \mathbf{U}_{pert} + (\mathbf{S}(\mathbf{U}) - \mathbf{S}(\bar{\mathbf{U}}) - \mathbf{S}'(\bar{\mathbf{U}}) \mathbf{U}_{pert}) =: \bar{\mathbf{S}} + \tilde{\mathbf{S}} + \hat{\mathbf{S}}. \end{aligned}$$

We, then, scale the components of the perturbation (see [18] for a discussion) by the scaling matrix $D := \operatorname{diag}(\varepsilon^{d_1}, \dots, \varepsilon^{d_q})$, and define the scaled perturbation as $\mathbf{V} := D^{-1} \mathbf{U}_{pert}$ to obtain the corresponding scaled splitting:

$$\mathbf{G} = \bar{\mathbf{G}} + \tilde{\mathbf{G}} + \hat{\mathbf{G}}, \quad \mathbf{Z} = \bar{\mathbf{Z}} + \tilde{\mathbf{Z}} + \hat{\mathbf{Z}},$$

with similar definitions as for the splittings of \mathbf{F} and \mathbf{S} . Defining $\mathbf{R} := -\operatorname{div}_x \mathbf{G} + \mathbf{Z}$ (with analogous definitions for $\bar{\mathbf{R}}, \tilde{\mathbf{R}}$ and $\hat{\mathbf{R}}$), and also $\bar{\mathbf{T}}$ as the (a priori-known) scaled residual of the reference solution

$$\bar{\mathbf{T}} := D^{-1} \partial_t \bar{\mathbf{U}} - \bar{\mathbf{R}}, \quad (2)$$

one can reformulate the balance laws (1) as

$$\partial_t \mathbf{V} = -\bar{\mathbf{T}} + \tilde{\mathbf{R}} + \hat{\mathbf{R}}, \quad (3)$$

which is a system for the scaled perturbation $\mathbf{V} := (v_1, \dots, v_q)^T$.

Solving this reformulated problem (3), numerically, defines the RS-IMEX scheme. We solve stiff $\tilde{\mathbf{R}}$ implicitly in time to avoid restrictive time steps in the limit (by using the implicit Euler method) while the (expected to be) non-stiff part $\hat{\mathbf{R}}$ is treated by the explicit Euler method. Moreover, $\bar{\mathbf{T}}$ is computed independently, e.g., by an incompressible solver if $\bar{\mathbf{U}}$ is the solution of the incompressible Euler equations. We use a Rusanov-type numerical flux, with numerical diffusion coefficients $\tilde{\alpha}$ and $\hat{\alpha}$ and an appropriate spatial discretization for the source term (to avoid well-balancing issues). Note that $\tilde{\alpha}$ and $\hat{\alpha}$ originally should be chosen as the maximum over the domain and all characteristic fields (of stiff or non-stiff parts). But here, not to add an excessive diffusion to the implicit step, we pick $\tilde{\alpha} = 0$.

Definition 1. Given the reference solution $\bar{\mathbf{U}}$, the RS-IMEX scheme for (3) is given by

$$D_t \mathbf{V}_\Delta^n = -\bar{\mathbf{T}}_\Delta^{n+1} + \tilde{\mathbf{R}}_\Delta^{n+1} + \hat{\mathbf{R}}_\Delta^n, \quad (4)$$

with the Euler time integration D_t when Δ stands for spatial discretization.

The advantages of the scheme are two-fold. Firstly, the implicit part of the scheme is linear by construction, which is very advantageous in terms of computational cost.¹ Secondly, as we will see in Remark 1, it makes the asymptotic consistency analysis easier as the scheme deals with the perturbations \mathbf{V} directly.

To summarize, in the RS-IMEX algorithm two coupled systems should be solved separately: with a given reference state at step n , one finds the scaled perturbation \mathbf{V}_Δ^{n+1} , while the reference state may evolve over time and should be computed independently. This procedure is repeated in each step.

2 RS-IMEX scheme for the shallow water equations

In this section, we apply the RS-IMEX scheme to the two-dimensional shallow water equations with bottom topography. Rather than the classical form of this system,

¹ The idea of such a linearization goes back to the so-called linearly-implicit methods for ODEs and has been used later in [2, 11].

we consider its reformulation as [2] in the periodic domain $\Omega = \mathbb{T}^2$:

$$\begin{cases} \partial_t z + \operatorname{div}_{\mathbf{x}} \mathbf{m} = 0, \\ \partial_t \mathbf{m} + \operatorname{div}_{\mathbf{x}} \left(\frac{\mathbf{m} \otimes \mathbf{m}}{z-b} + \frac{z^2 - 2bz}{2\varepsilon^2} \mathbb{I}_2 \right) = -\frac{z}{\varepsilon^2} \nabla_{\mathbf{x}} b, \end{cases} \quad (5)$$

where z is the surface elevation from the mean surface level H_{mean} , $\mathbf{m} := (z-b)\mathbf{u}$ is the momentum with the velocity $\mathbf{u} = (u_1, u_2)$, b is the water depth measured from H_{mean} with a negative sign, and the singular parameter $\varepsilon \in (0, 1]$ is called the Froude number, cf. [18]. Using (5), one can identify \mathbf{U} , \mathbf{F} and \mathbf{S} as

$$\mathbf{U} = \begin{bmatrix} z \\ m_1 \\ m_2 \end{bmatrix}, \quad \mathbf{F} = \begin{bmatrix} m_1 & m_2 \\ \frac{m_1^2}{z-b} + \frac{z^2 - 2zb}{2\varepsilon^2} & \frac{m_1 m_2}{z-b} \\ \frac{m_1 m_2}{z-b} & \frac{m_2^2}{z-b} + \frac{z^2 - 2zb}{2\varepsilon^2} \end{bmatrix}, \quad \mathbf{S} = \begin{bmatrix} 0 \\ -zb_x/\varepsilon^2 \\ -zb_y/\varepsilon^2 \end{bmatrix}. \quad (6)$$

Given the scaling matrix $D = \operatorname{diag}(\varepsilon^2, 1, 1)$, $\bar{\mathbf{U}} = (\bar{z}, \bar{m}_1, \bar{m}_2)^T$, and the scaled perturbation $\mathbf{V} := D^{-1}(\mathbf{U} - \bar{\mathbf{U}})$, the RS-IMEX splitting for (5) gives the reference and stiff parts as

$$\bar{\mathbf{G}} = \begin{bmatrix} \frac{\bar{m}_1/\varepsilon^2}{\frac{\bar{m}_1^2}{\bar{z}-b} + \frac{\bar{z}^2 - 2\bar{z}b}{2\varepsilon^2}} & \frac{\bar{m}_2/\varepsilon^2}{\frac{\bar{m}_1 m_2}{\bar{z}-b}} \\ \frac{\bar{m}_1 m_2}{\bar{z}-b} & \frac{\bar{m}_2^2}{\bar{z}-b} + \frac{\bar{z}^2 - 2\bar{z}b}{2\varepsilon^2} \end{bmatrix}, \quad (7a)$$

$$\tilde{\mathbf{G}} = \begin{bmatrix} \frac{v_2/\varepsilon^2}{-\frac{\bar{m}_1^2 v_1 \varepsilon^2}{(\bar{z}-b)^2} + \frac{2\bar{m}_1 v_2}{\bar{z}-b} + (\bar{z}-b)v_1} & \frac{v_3/\varepsilon^2}{-\frac{\bar{m}_1 m_2 v_1 \varepsilon^2}{(\bar{z}-b)^2} + \frac{\bar{m}_1 v_3}{\bar{z}-b} + \frac{\bar{m}_2 v_2}{\bar{z}-b}} \\ -\frac{\bar{m}_1 m_2 v_1 \varepsilon^2}{(\bar{z}-b)^2} + \frac{\bar{m}_1 v_3}{\bar{z}-b} + \frac{\bar{m}_2 v_2}{\bar{z}-b} & -\frac{\bar{m}_2^2 v_1 \varepsilon^2}{(\bar{z}-b)^2} + \frac{2\bar{m}_2 v_3}{\bar{z}-b} + (\bar{z}-b)v_1 \end{bmatrix}, \quad (7b)$$

$$\bar{\mathbf{Z}} = \begin{bmatrix} 0 \\ -\bar{z}b_x/\varepsilon^2 \\ -\bar{z}b_y/\varepsilon^2 \end{bmatrix}, \quad \tilde{\mathbf{Z}} = \begin{bmatrix} 0 \\ -v_1 b_x \\ -v_1 b_y \end{bmatrix}. \quad (7c)$$

while $\hat{\mathbf{Z}} = \mathbf{0}$ and $\hat{\mathbf{G}}(\bar{\mathbf{U}}, \mathbf{V}) = \mathbf{G}(\bar{\mathbf{U}} + \mathbf{V}) - \bar{\mathbf{G}}(\bar{\mathbf{U}}) - \tilde{\mathbf{G}}(\bar{\mathbf{U}}, \mathbf{V})$. One can verify that the Jacobian matrices $\hat{\mathbf{G}}'$ and $\tilde{\mathbf{G}}'$ have complete sets of eigenvectors and that the eigenvalues of $\hat{\mathbf{G}}'$ are non-stiff. This can be readily seen from the expression of the non-stiff flux $\hat{\mathbf{G}}_1$ (and similarly $\hat{\mathbf{G}}_2$)

$$\widehat{\mathbf{G}}_1 = \begin{bmatrix} 0 \\ \frac{m_1^2}{z-b} + \frac{z^2 - 2zb}{2\varepsilon^2} - \frac{\bar{m}_1^2}{\bar{z}-b} - \frac{\bar{z}^2 - 2\bar{z}b}{2\varepsilon^2} + \frac{\bar{m}_1^2 v_1 \varepsilon^2}{(\bar{z}-b)^2} - \frac{2\bar{m}_1 v_2}{\bar{z}-b} - (\bar{z}-b)v_1 \\ \frac{m_1 m_2}{z-b} - \frac{\bar{m}_1 \bar{m}_2}{\bar{z}-b} + \frac{\bar{m}_1 \bar{m}_2 v_1 \varepsilon^2}{(\bar{z}-b)^2} - \frac{\bar{m}_1 v_3}{\bar{z}-b} - \frac{\bar{m}_2 v_2}{\bar{z}-b} \end{bmatrix}, \quad (7d)$$

as, after simplification, it does not contain any $\mathcal{O}(1/\varepsilon)$ term.

Denoting the central discretization of the first and second derivatives in the x -direction by $\nabla_{h,x}$ and $\Delta_{h,x}$ respectively, the RS-IMEX scheme can be written as

$$\mathbf{V}_{ij}^{n+1/2} = \mathbf{V}_{ij}^n - \Delta t \left(\nabla_{h,x} \widehat{\mathbf{G}}_{1,ij}^n + \nabla_{h,y} \widehat{\mathbf{G}}_{2,ij}^n \right) + \Delta t \frac{\widehat{\alpha} \Delta x}{2} \Delta_{h,x} \mathbf{V}_{ij}^n, \quad (8a)$$

$$\mathbf{V}_{ij}^{n+1} = \mathbf{V}_{ij}^{n+1/2} - \Delta t \left(\nabla_{h,x} \widetilde{\mathbf{G}}_{1,ij}^{n+1} + \nabla_{h,y} \widetilde{\mathbf{G}}_{2,ij}^{n+1} \right) + \Delta t \widetilde{\mathbf{Z}}_{ij}^{n+1} - \Delta t \bar{\mathbf{T}}_{ij}^{n+1}, \quad (8b)$$

for each cell $(i, j) \in \{1, 2, \dots, N\}^2$ in the square computational domain Ω_N with spatial steps $\Delta x = \Delta y$ and the time step Δt , where $\widetilde{\mathbf{Z}}_{ij}^{n+1}$ is the central discretization of the source term (7c), and $\bar{\mathbf{T}}_{ij}^{n+1}$ is the discretization of the scaled residual (2) computed as (with $\bar{\alpha} = 0$)

$$\bar{\mathbf{T}}_{ij}^{n+1} = D^{-1} \frac{\bar{\mathbf{U}}_{ij}^{n+1} - \bar{\mathbf{U}}_{ij}^n}{\Delta t} + \nabla_{h,x} \bar{\mathbf{G}}_{1,ij}^{n+1} + \nabla_{h,y} \bar{\mathbf{G}}_{2,ij}^{n+1} - \bar{\mathbf{Z}}_{ij}^{n+1}. \quad (9)$$

The reference solution is chosen as the zero-Froude limit, which is the solution of the so-called *lake equations* (cf. [3] for a formal derivation):

$$\begin{cases} \partial_t \mathbf{m} - \operatorname{div}_x \left(\frac{\mathbf{m} \otimes \mathbf{m}}{b} \right) - b \nabla_x \pi = \mathbf{0}, \\ \operatorname{div}_x \mathbf{m} = 0. \end{cases} \quad (10)$$

So, considering the solution of (10) as $\bar{\mathbf{U}}$ with a constant (in time and space) \bar{z} and a solenoidal $\bar{\mathbf{m}}$, one can write $\bar{\mathbf{T}}$ block-wise as $\bar{\mathbf{T}}_{\Delta}^{n+1} := [\bar{\mathbf{T}}_{1,\Delta}^{n+1}, \bar{\mathbf{T}}_{2,\Delta}^{n+1}, \bar{\mathbf{T}}_{3,\Delta}^{n+1}]^T$ with

$$\begin{aligned} \bar{\mathbf{T}}_{1,ij}^{n+1} &= \left(\nabla_{h,x} \bar{m}_{1,ij}^{n+1} + \nabla_{h,x} \bar{m}_{2,ij}^{n+1} \right) / \varepsilon^2, \\ \bar{\mathbf{T}}_{2,ij}^{n+1} &= D_t \bar{m}_{1,ij}^n + \nabla_{h,x} \left(\frac{\bar{m}_{1,ij}^{n+1,2}}{\bar{z} - b_{ij}} \right) + \nabla_{h,y} \left(\frac{\bar{m}_{1,ij}^{n+1} \bar{m}_{2,ij}^{n+1}}{\bar{z} - b_{ij}} \right), \\ \bar{\mathbf{T}}_{3,ij}^{n+1} &= D_t \bar{m}_{2,ij}^n + \nabla_{h,x} \left(\frac{\bar{m}_{1,ij}^{n+1} \bar{m}_{2,ij}^{n+1}}{\bar{z} - b_{ij}} \right) + \nabla_{h,y} \left(\frac{\bar{m}_{1,ij}^{n+1,2}}{\bar{z} - b_{ij}} \right). \end{aligned} \quad (11)$$

So far, the scheme for computing the scaled perturbation has been introduced. The remaining point to be clarified is how to solve the equations for the reference solution (10), which is needed to compute $\bar{\mathbf{T}}$. In fact, there exist several numerical

methods for the lake equations. Here, we employ the so-called Chorin's *projection method* [4] because of its simplicity and applicability to collocated grids. We wish to mention that the Poisson problem (in the projection method) for a doubly-periodic domain has an infinite number of solutions differed by a constant. To solve it numerically we use the Discrete Fourier Transform (DFT) for the flat bottom case, while for the non-flat bottom case, we regularize the problem by a time derivative in the pseudo time τ and seek the stationary solution.

3 Main result: asymptotic analysis of the scheme

Theorem 1. *Consider the shallow water equations (5) with topography in a periodic domain and with well-prepared initial data $(z_{0,\varepsilon}, \mathbf{m}_{0,\varepsilon})$ such that*

$$z(0, \cdot) = z_{0,\varepsilon} = z_{(0)}^0 + \varepsilon^2 z_{(2),\varepsilon}^0, \quad \mathbf{m}(0, \cdot) = \mathbf{m}_{0,\varepsilon} = \mathbf{m}_{(0)}^0 + \varepsilon \mathbf{m}_{(1),\varepsilon}^0,$$

where $z_{(0)}^0$ is a constant and $\mathbf{m}_{(0)}^0$ satisfies the lake equations (10). Then, the RS-IMEX scheme (8a)–(8b) is solvable, i.e., it has a unique solution for all $\varepsilon > 0$, if $\tilde{\alpha}$ is constant. Also, the scheme is consistent with the asymptotic limit in the fully-discrete settings, i.e., it is asymptotically consistent.

3.1 Solvability

Assuming $\Delta x = \Delta y$ and $\tilde{\alpha} = 0$ for simplicity, the linear system of the implicit step (8b) with the companion matrix J_ε can be written as $J_\varepsilon := \mathbb{I}_{3N^2} + \beta \Xi_\varepsilon$, where $\beta := \frac{\Delta t}{2\Delta x}$ and Ξ_ε is a matrix not depending on β . It is plausible to conclude that for a suitable choice of β , none of the eigenvalues of $\beta \Xi_\varepsilon$ is equal to -1 ; so J_ε is non-singular, and the implicit step (so the whole scheme) is solvable. The proof for $\tilde{\alpha} \neq 0$ is likewise.

3.2 Asymptotic consistency

The asymptotic consistency analysis is often done formally in the literature, namely by putting the Poincaré expansion ansatz into the scheme and balancing the equal powers of ε . For the present work, we adopt the same approach.

Firstly, we show that the explicit step is “ ε -stable”, i.e., $\|\mathbf{V}_\Delta^{n+1/2}\| = \mathcal{O}(1)$. Given $\|\mathbf{V}_\Delta^n\| = \mathcal{O}(1)$, which is compatible with the well-prepared initial data, and since $\widehat{\mathbf{G}}_{1,1} = \widehat{\mathbf{G}}_{2,1} = 0$, one can immediately conclude that $\|\mathbf{V}_{1,\Delta}^{n+1/2}\| = \mathcal{O}(1)$. For $\mathbf{V}_{2,\Delta}$ (and similarly $\mathbf{V}_{3,\Delta}$), one can simply confirm that

$$\lim_{\varepsilon \rightarrow 0} \left(\nabla_{h,x} \widehat{\mathbf{G}}_{1,2,ij}^n + \nabla_{h,y} \widehat{\mathbf{G}}_{2,2,ij}^n \right) = \mathcal{O}(1), \quad (12)$$

since

$$\begin{aligned} \lim_{\varepsilon \rightarrow 0} \left[\nabla_{h,x} \left(\frac{m_1^2}{z-b} + \frac{z^2 - 2zb}{2\varepsilon^2} - \frac{\overline{m}_1^2}{\bar{z}-b} - \frac{\bar{z}^2 - 2\bar{z}b}{2\varepsilon^2} + \frac{\overline{m}_1^2 v_1 \varepsilon^2}{(\bar{z}-b)^2} - \frac{2\overline{m}_1 v_2}{\bar{z}-b} - (\bar{z}-b)v_1 \right) \right. \\ \left. + \nabla_{h,y} \left(\frac{m_1 m_2}{z-b} - \frac{\overline{m}_1 \overline{m}_2}{\bar{z}-b} + \frac{\overline{m}_1 \overline{m}_2 v_1 \varepsilon^2}{(\bar{z}-b)^2} - \frac{\overline{m}_1 v_3}{\bar{z}-b} - \frac{\overline{m}_2 v_2}{\bar{z}-b} \right) \right] = \mathcal{O}(1). \end{aligned}$$

So, the explicit step does not change the leading order of $\mathbf{V}_{2,\Delta}^n$ (and $\mathbf{V}_{3,\Delta}^n$). This concludes the ε -stability proof of the explicit step.

Completing the asymptotic consistency analysis, we show that the implicit step is consistent with the limit. We *assume* that $\|\mathbf{V}_{\Delta}^{n+1}\| = \mathcal{O}(1)$ to justify the use of Poincaré expansion and will discuss this assumption somewhere else. From the v_1 -update, (11) and (7a)–(7d), the momentum field (up to $\mathcal{O}(\varepsilon^2)$) is solenoidal, i.e.,

$$\nabla_{h,x} (\overline{m}_1 + v_2)_{ij}^{n+1} + \nabla_{h,y} (\overline{m}_2 + v_3)_{ij}^{n+1} = \mathcal{O}(\varepsilon^2). \quad (13)$$

Since the consistency of the evolution of the leading order of the momentum is clear, the asymptotic consistency of the scheme is concluded, but only up to possible oscillations for the momentum field in the null space of central difference operators $\nabla_{h,x}$ and $\nabla_{h,y}$ which may lead to checker-board oscillations.

Remark 1. The equation (13), combined with the v_1 -update, immediately implies that possible checker-board oscillations for the surface perturbation z are small, i.e., $\mathcal{O}(\varepsilon^2)$. This seems to solve the problem in [15] regarding the checker-board oscillations in a periodic domain, and suggests that it may not be necessary to add a large diffusion in order to preclude oscillations.

4 Numerical results

We discuss the traveling vortex example [2] to verify the quality of the solutions computed by the RS-IMEX scheme. We consider a well-prepared initial condition in the periodic domain $\Omega = [0, 1)^2$:

$$\begin{aligned} z(x, y, 0) &= \mathbf{1}_{[r \leq \frac{\pi}{\omega}]} \left(\frac{\Gamma \varepsilon}{\omega} \right)^2 (g(\omega r) - g(\pi)), \\ u_1(x, y, 0) &= u_0 + \mathbf{1}_{[r \leq \frac{\pi}{\omega}]} \Gamma (1 + \cos(\omega r)) (y_c - y), \\ u_2(x, y, 0) &= \mathbf{1}_{[r \leq \frac{\pi}{\omega}]} \Gamma (1 + \cos(\omega r)) (x - x_c), \end{aligned}$$

with $H_{mean} = 110$, $u_0 = 0.6$, $\mathbf{x}_c = (0.5, 0.5)^T$, $\Gamma = 1.4$, $\omega = 4\pi$, $r := \|\mathbf{x} - \mathbf{x}_c\|$ and

$$g(r) := 2 \cos r + 2r \sin r + \frac{1}{8} \cos 2r + \frac{r}{4} \sin 2r + \frac{3}{4} r^2.$$

We choose the time step as $\Delta t := \text{CFL} \Delta x / \hat{\alpha}$. The exact solution is the initial condition advected by u_0 with time-periodicity $T_\pi = \frac{5}{3}$ such that $w(x, y, t) = w(x - u_0 t, y, 0)$ for $w \in \{z, u_1, u_2\}$. Using this exact solution, Table 1 shows the experimental order of convergence (EOC) for the final time $T_f = 1$ and for different ε ; it is clear that the EOC is close to one uniformly in ε and the scheme is accurate for all $\varepsilon > 0$. We also illustrate this fact in Figure 1, where both exact and numerical solutions are plotted on centerlines of the domain.

Table 1: Experimental order of convergence with CFL = 0.45 and for different ε . Error e is defined with the exact solution in ℓ_∞ -norm.

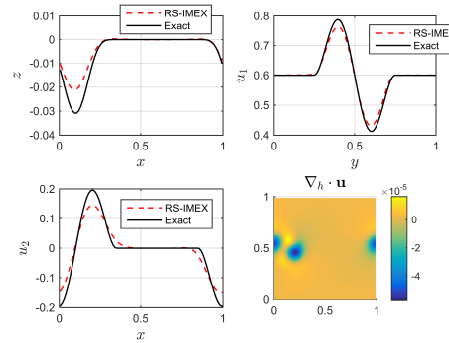
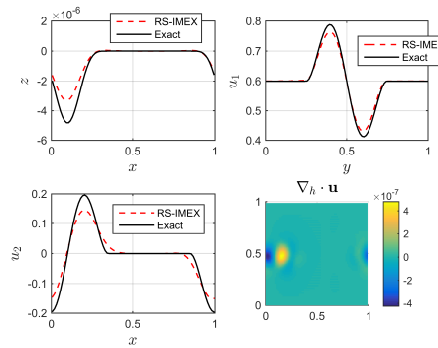
N	$\varepsilon = 0.8$				N	$\varepsilon = 10^{-6}$			
	e_{z, ℓ_∞}	EOC_{z, ℓ_∞}	e_{u_1, ℓ_∞}	EOC_{u_1, ℓ_∞}		e_{z, ℓ_∞}	EOC_{z, ℓ_∞}	e_{u_1, ℓ_∞}	EOC_{u_1, ℓ_∞}
20	2.61e-2	-	1.04e-1	-	20	4.08e-14	-	1.04e-1	-
40	2.00e-2	0.38	6.80e-2	0.61	40	3.13e-14	0.38	6.80e-2	0.61
80	1.23e-2	0.70	3.63e-2	0.91	80	1.92e-14	0.71	3.63e-2	0.91
160	6.20e-3	0.99	1.65e-3	1.14	160	9.69e-15	0.99	1.65e-3	1.14

Figure 2a illustrates the computed solution for a small ε , in particular $\varepsilon = 10^{-6}$. There is a very good agreement between the result of the RS-IMEX scheme and the exact solution. It is also clear that there is no checker-board oscillation for the momentum and surface perturbation. These suggest that the scheme is asymptotically consistent and stable. Moreover, Figure 2b shows that the scaled perturbation is bounded in terms of ε ; so, the formal asymptotic consistency analysis is justified.

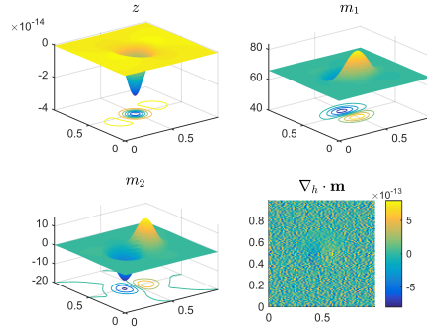
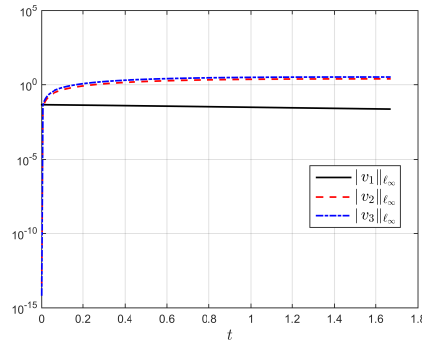
Acknowledgements The research was supported by RWTH Aachen University through *Graduiertenförderung nach Richtlinien zur Förderung des wissenschaftlichen Nachwuchses (RFwN)*.

References

1. G. BISPEN, *IMEX finite volume methods for the shallow water equations*, PhD thesis, Johannes Gutenberg-Universität, 2015.
2. G. BISPEN, K. R. ARUN, M. LUKÁČOVÁ-MEDVID'OVÁ, AND S. NOELLE, *IMEX large time step finite volume methods for low Froude number shallow water flows*, Communication in Computational Physics, 16 (2014), pp. 307–347.
3. D. BRESCH, R. KLEIN, AND C. LUCAS, *Multiscale analyses for the shallow water equations*, in Computational Science and High Performance Computing IV, Springer, 2011, pp. 149–164.
4. A. J. CHORIN, *Numerical solution of the Navier–Stokes equations*, Mathematics of Computation, 22 (1968), pp. 745–762.
5. P. DEGOND AND M. TANG, *All speed scheme for the low Mach number limit of the isentropic Euler equation*, Communications in Computational Physics, 10 (2011), pp. 1–31.
6. S. DELLACHERIE, *Analysis of Godunov type schemes applied to the compressible Euler system at low Mach number*, Journal of Computational Physics, 229 (2010), pp. 978–1016.

(a) $\varepsilon = 0.8$.(b) $\varepsilon = 0.01$.Fig. 1: Error of the RS-IMEX scheme for different ε on the 80×80 grid, with $\text{CFL} = 0.45$ and $T_f = 1$.

7. L. EVEN-DAR MANDEL AND S. SCHOCHET, *Convergence of solutions to finite difference schemes for singular limits of nonlinear evolutionary PDEs*, ESAIM: Mathematical Modelling and Numerical Analysis-Modélisation Mathématique et Analyse Numérique, (2016). doi: 10.1051/m2an/2016029.
8. ———, *Uniform discrete Sobolev estimates of solutions to finite difference schemes for singular limits of nonlinear PDEs*, ESAIM: Mathematical Modelling and Numerical Analysis-Modélisation Mathématique et Analyse Numérique, (2016). doi: 10.1051/m2an/2016038.
9. F. FILBET AND S. JIN, *A class of asymptotic-preserving schemes for kinetic equations and related problems with stiff sources*, Journal of Computational Physics, 229 (2010), pp. 7625–7648.
10. J. GIESSELMANN, *Low Mach asymptotic-preserving scheme for the Euler–Korteweg model*, IMA Journal of Numerical Analysis, 35 (2015), pp. 802–833.
11. F. X. GIRALDO AND M. RESTELLI, *High-order semi-implicit time-integrators for a triangular discontinuous Galerkin oceanic shallow water model*, International Journal for Numerical Methods in Fluids, 63 (2010), pp. 1077–1102.
12. J. HAACK, S. JIN, AND J.-G. LIU, *An all-speed asymptotic-preserving method for the isentropic Euler and Navier–Stokes equations*, Communications in Computational Physics, 12 (2012), pp. 955–980.
13. S. JIN, *Efficient asymptotic-preserving (AP) schemes for some multiscale kinetic equations*, SIAM Journal on Scientific Computing, 21 (1999), pp. 441–454.

(a) Solution of the RS-IMEX scheme for $\varepsilon = 10^{-6}$.(b) Time evolution of the norm of the perturbation from the incompressible solution for $\varepsilon = 10^{-6}$. The figure is almost the same for $\varepsilon = 10^{-4}$ and $\varepsilon = 10^{-2}$.Fig. 2: Behaviour of the scheme on the 100×100 grid with $\text{CFL} = 0.45$ and $T_f = T_\pi$.

14. ———, *Asymptotic preserving (AP) schemes for multiscale kinetic and hyperbolic equations: A review*, Lecture Notes for Summer School on “Methods and Models of Kinetic Theory” (M&MKT), Porto Ercole (Grosseto, Italy), (2010), pp. 177–216.
15. K. KAISER, J. SCHÜTZ, R. SCHÖBEL, AND S. NOELLE, *A new stable splitting for the isentropic Euler equations*, Journal of Scientific Computing, (2016), pp. 1–18.
16. N. MASMOUDI, *Examples of singular limits in hydrodynamics*, Handbook of Differential Equations: Evolutionary Equations, 3 (2007), pp. 195–275.
17. S. NOELLE, G. BISPEN, K. R. ARUN, M. LUKÁČOVÁ-MEDVID’OVÁ, AND C.-D. MUNZ, *A weakly asymptotic preserving low Mach number scheme for the Euler equations of gas dynamics*, SIAM Journal on Scientific Computing, 36 (2014), pp. B989–B1024.
18. H. ZAKERZADEH, *Asymptotic analysis of the RS-IMEX scheme for the shallow water equations in one space dimension*, HAL: hal-01491450, (2016). IGPM report 455, RWTH Aachen University, Submitted for publication.
19. ———, *On the Mach-uniformity of the Lagrange-projection scheme*, ESAIM: Mathematical Modelling and Numerical Analysis-Modélisation Mathématique et Analyse Numérique, (2016). 10.1051/m2an/2016064.